New Phytologist

Brassinosteroid production and signaling differentially control cell division and expansion in the leaf

Miroslava K. Zhiponova[1,2], Isabelle Vanhoutte[1,2], Véronique Boudolf[1,2], Camilla Betti[1,2], Stijn Dhondt[1,2], Frederik Coppens[1,2], Evelien Mylle[1,2], Sara Maes[1,2], Mary-Paz González-García[3], Ana I. Caño-Delgado[3], Dirk Inzé[1,2], Gerrit T. S. Beemster[4], Lieven De Veylder[1,2] and Eugenia Russinova[1,2]

[1]Department of Plant Systems Biology, VIB, B-9052, Ghent, Belgium; [2]Department of Plant Biotechnology and Bioinformatics, Ghent University, B-9052, Ghent, Belgium; [3]Molecular Genetics Department, Centre for Research in Agricultural Genomics CSIC-IRTA-UAB, 08013, Barcelona, Spain; [4]Department of Biology, University of Antwerp, B-2020, Antwerp, Belgium

Author for correspondence:
Eugenia Russinova
Tel:+32 9 331 39 31
Email: jenny.russinova@psb.vib-ugent.be

Received: *13 August 2012*
Accepted: *7 October 2012*

New Phytologist (2013) **197:** 490–502
doi: 10.1111/nph.12036

Key words: Arabidopsis, brassinosteroids, cell division, *cpd*, leaf.

Summary

- Brassinosteroid (BR) hormones control plant growth through acting on both cell expansion and division. Here, we examined the role of BRs in leaf growth using the Arabidopsis BR-deficient mutant *constitutive photomorphogenesis and dwarfism* (*cpd*).
- We show that the reduced size of *cpd* leaf blades is a result of a decrease in cell size and number, as well as in venation length and complexity. Kinematic growth analysis and tissue-specific marker gene expression revealed that the leaf phenotype of *cpd* is associated with a prolonged cell division phase and delayed differentiation.
- *cpd*-leaf-rescue experiments and leaf growth analysis of BR biosynthesis and signaling gain-of-function mutants showed that BR production and BR receptor-dependent signaling differentially control the balance between cell division and expansion in the leaf.
- Investigation of cell cycle markers in leaves of *cpd* revealed the accumulation of mitotic proteins independent of transcription. This correlated with an increase in cyclin-dependent kinase activity, suggesting a role for BRs in control of mitosis.

Introduction

In Arabidopsis, leaves are initiated at the flanks of the shoot apical meristem by cell division, followed by gradual (tip to the base) maturation marked by cell cycle exit and cell expansion (Donnelly *et al.*, 1999; Efroni *et al.*, 2010; Andriankaja *et al.*, 2012). Genetic, hormonal and environmental factors control leaf growth and development (Tsukaya, 2002; Bögre *et al.*, 2008; Skirycz & Inzé, 2010). Brassinosteroid (BR) hormones are known to be essential for leaf growth because BR loss-of-function mutants display severe leaf phenotypes including small, round-shaped leaves and short petioles (Clouse *et al.*, 1996; Szekeres *et al.*, 1996; Li & Chory, 1997; Choe *et al.*, 1998; Friedrichsen *et al.*, 2000; Li *et al.*, 2001). Conversely, BR gain-of-function mutants show larger and elongated leaf blades and longer petioles (Choe *et al.*, 2001; Wang *et al.*, 2001; Yin *et al.*, 2002; Gonzalez *et al.*, 2010; Oh *et al.*, 2011). The dwarf leaf phenotype of the BR loss-of-function mutants is attributed mainly to impaired cell expansion because of the smaller cell size of these mutants (Chory *et al.*, 1991; Clouse *et al.*, 1996; Kauschmann *et al.*, 1996; Szekeres *et al.*, 1996; Fujioka *et al.*, 1997; Azpiroz *et al.*, 1998; Choe *et al.*, 1999). However, exogenous BRs rescue the leaf size of the *de-etiolated2* (*det2*) mutant, defective in the biosynthesis of BRs, by increasing both mesophyll cell size and number, implying that BRs promote leaf growth by positively regulating both cell expansion and cell division (Nakaya *et al.*, 2002). In agreement with this conclusion, the enlarged leaf size of Arabidopsis plants overexpressing the BR receptor *BR INSENSITIVE 1* (*BRI1*) and the gain-of-function phosphorylation mutant *BRI1* (*Y831F*) is a result of an increase in the epidermal cell number (Gonzalez *et al.*, 2010; Oh *et al.*, 2011), suggesting that BRs promote cell division during leaf growth. A short-term promotion of cell division by BRs is also observed in tobacco (*Nicotiana tabacum)* protoplasts and Bright Yellow-2 (BY-2) cells (Nakajima *et al.*, 1996; Oh & Clouse, 1998; Miyazawa *et al.*, 2003), whereas impaired BR biosynthesis in callus cells of Arabidopsis results in slower cell division rates (Cheon *et al.*, 2010). Also, the short root phenotype of the null BR receptor mutant *bri1-116* is caused by defects in both cell expansion and in the cell cycle progression in the root meristem (González-García *et al.*, 2011; Hacham *et al.*, 2011).

To date, the mechanism of BR-mediated control of cell division remains elusive. Several reports have shown that BRs enhance the transcription of core cell cycle genes such as *CYCLIN D3* (*CYCD3*), *CYCLIN B1;1* (*CYCB1;1*), *HISTONE 4* (*H4*) and the B-type *CYCLIN-DEPENDENT KINASE B1;1* (*CDKB1;1*) in Arabidopsis plants, cultures, and BY-2 cells (Yoshizumi *et al.*, 1999; Hu *et al.*, 2000; Miyazawa *et al.*, 2003). Conversely, BR loss-of-function mutants display a reduced expression of *CYCB1;1* and an increased expression of the cell cycle inhibitor *KIP-RELATED PROTEIN 2* (*KRP2*) (González-García *et al.*, 2011; Hacham *et al.*, 2011). Identification of several cell cycle genes as direct targets of both the

BRASSINAZOLE RESISTANT 1 (BRZ1) and the BRI1 EMS SUPPRESSOR 1 (BES1)/BZR2 transcription factors might imply a transcriptional control of the cell cycle by BRs (Sun *et al.*, 2010; Gudesblat & Russinova, 2011; Yu *et al.*, 2011).

In addition to cell cycle progression, BRs are required for differentiation of the cells in the leaf margin (Reinhardt *et al.*, 2007) and for defining the timing of differentiation in the root (González-García *et al.*, 2011). BRs also control the differentiation of vascular tissues in the shoot, as Arabidopsis and rice (*Oryza sativa*) BR loss-of-function mutants have less xylem (Caño-Delgado *et al.*, 2004; Nakamura *et al.*, 2006; Ibañes *et al.*, 2009).

To understand how BRs promote leaf growth, we analyzed cell division, expansion, and differentiation in Arabidopsis leaves of the BR-deficient mutant *constitutive photomorphogenesis and dwarfism* (*cpd*). We provide evidence that BRs are essential for cell cycle progression during leaf growth. *cpd*-rescue experiments and investigation of BR biosynthesis and signaling gain-of-function mutants show that BR production and BR receptor-dependent signaling have distinct effects on cell division and expansion in the leaf. Several mitotic proteins accumulated in *cpd* mutants independent of transcription. This correlated with an increase in cyclin-dependent kinase activity, suggesting the hypothesis that BRs are required for the degradation of mitotic regulators.

Materials and Methods

Plant material, marker lines and growth conditions

Arabidopsis thaliana (L.) Heynh. ecotype Columbia-0 (Col-0) plants and mutants in the same genetic background were used except for the *Pro35S:CYCD3;1* (*CYCD3;1*^{OE}) transgenic line (Dewitte *et al.*, 2003), which was in the Landsberg erecta ecotype. *cpd* (Szekeres *et al.*, 1996), *bri1-116*, and *ProBRI1:BRI1-GFP* (*BRI1*^{OE}) (Friedrichsen *et al.*, 2000) were crossed with the following transcriptional or translational reporters: *ProCYCA2;1:GUS* (Vanneste *et al.*, 2011), *ProCYCB1;1:GUS* (De Smet *et al.*, 2008), *ProCYCB1;1:DB-GUS* (Colón-Carmona *et al.*, 1999), *ProCYCB1;2:DB-GUS* (Schnittger *et al.*, 2002), *Pro35S:GFP-TUB6* (Nakamura *et al.*, 2004), *ProATHB15:nlsYFP* (nls-nuclear localization signal), *ProPIN1:GUS* (Friml *et al.*, 2003), and *ProDR5:GUS* (Ulmasov *et al.*, 1997). The *ProATHB15:nlsYFP* construct contained the 2-kb promoter fragment of the *ATHB15* gene cloned in the pDONRTM-221 vector and later in the pBGYN binary vector using Gateway® cloning technology (Invitrogen, Carlsbad, CA, USA; Supporting Information Table S1). These constructs were introduced into *Agrobacterium tumefaciens* C58pMP90 and transformed into Col-0 plants by floral dipping (Clough & Bent, 1998). The mutant *Pro35S-DWF4* (*DWF4*^{OE}) (Wang *et al.*, 2001) was also used. Transgenic lines and mutants were genotyped using primers listed in Table S1.

Before transfer to the light, seeds were incubated in the dark at 4°C for 48 h. Plants were grown under standard growth conditions (21°C; 16 h : 8 h, light : dark photoperiod) on vertical plates containing half-strength Murashige and Skoog medium supplemented with 0.8% plant tissue culture agar (LAB M Ltd, Heywood, UK) and 1% sucrose. The *bri1-116* and *BRI1*^{OE} mutants were grown in growth chambers (21°C; 16 h : 8 h, light : dark photoperiod; light intensity 100 μmol m^{-2} s^{-1} photosynthetically active radiation; 55% humidity), in peat pellets (Jiffy International As, Stange, Norway). The *cpd*-rescue experiment was performed at 8 d after sowing (DAS) *in vitro* on medium supplemented with dimethylsulfoxide (DMSO) for the mock treatments, or with 100 nM BL (Wako Pure Chemical Industries, Osaka, Japan). The vertical-grown plants at 8 DAS were transferred to DMSO- or BL-containing medium in sterile conditions. To avoid contact with the agar, the rosettes were placed on sterile parafilm strips, whereas the roots were kept in contact with the medium.

Growth analysis

Leaves were harvested and cleared in the following series of solutions: absolute ethanol (1–2 d), 1.25 M NaOH : EtOH (1 : 1 v/v) solution for 2 h at 60°C, lactic acid saturated in chloral hydrate, and finally lactic acid. The leaves were mounted on microscopic slides with the abaxial side upwards. Whole leaves were photographed using a Nikon camera connected to a binocular MZ16 Leica microscope for subsequent measuring of the leaf blade area with ImageJ software (Abràmoff *et al.*, 2004). Cells at the abaxial epidermis and the palisade mesophyll were imaged using differential interference contrast (DIC) BX51 microscopes (Olympus Europa, Munich, Germany) at 25% (leaf base) and 75% (leaf base) of the leaf blade length. The number of cells (50 cells on average) per drawn image area was counted in ImageJ and extrapolated to the whole leaf area. The average cell size at the leaf base and tip was calculated from the ratio of image area/cell number. In total eight leaves per genotype or treatment were analyzed and at least two independent experiments were performed. The kinematic analysis was performed according to De Veylder *et al.* (2001) and Achard *et al.* (2009). A detailed description of the venation pattern analysis methods is given in Dhondt *et al.* (2012). The following parameters characterizing the venation pattern were measured: number of areolas (i.e. the area closed by vasculature), the number of branching points (where a vein is crossed by another vein), the number of end points (where a vein stops), and venation pattern complexity (i.e. the sum of the number of all branching and endpoints, and the connections between the veins).

Pavement cell circularity was extracted automatically from the epidermal microscopic drawings using an ImageJ macro. Circularity was calculated according to the following formula: $4\pi A/P^2$, where A is the area and P is the perimeter of the cell. A circularity value of 1 represents a perfect circular morphology, and a value of 0 indicates an elongated polygon.

The percentage of mitotic events visualized using TUBULIN6 (TUB6)- and CYCB1;2-positive cells (M cells) per total mesophyll cell number was calculated according to Donnelly *et al.* (1999). To measure the frequency of mitotic events and M cells at the tip and the base of the leaf, 100 cells per region were taken and the respective ratios (mitotic events per 100 cells, and M cells per 100 cells) were calculated.

Flow cytometry

For flow cytometry, frozen leaves were chopped with a razor blade in 200 µl of Cystain UV Precise P Nuclei extraction buffer followed by the addition of 800 µl of staining buffer (buffers from Partec, Münster, Germany), and the mix was filtered through a 50-µm mesh. The distribution of the nuclear DNA content was analyzed using a CytoFlow ML flowcytometer and FloMax software (Partec, Münster, Germany).

Confocal microscopy

Transgenic Arabidopsis leaves were assayed for GFP and YFP fluorescence either with a 100 M Zeiss confocal microscope with software package LSM 510 version 3.2 or with an Olympus FluoView FV1000 microscope equipped with a ×63 water-corrected objective (numerical aperture of 1.2). The GFP fluorescence was excited with a 488-nm laser. Emission fluorescence was captured in the frame-scanning mode alternating GFP fluorescence via a 500–550-nm band-pass filter.

GUS assay

For analysis of GUS activity, plants were submerged in 90% acetone for 30 min at 4°C, washed once with phosphate buffer (pH 7) at room temperature and incubated in GUS solution (1 mM X-Glc; 0.5% dimethylformamide, 0.5% Triton X-100, 1 mM EDTA, 0.5 mM K3Fe(CN)6 and 0.5 mM K4Fe(CN)6 in phosphate buffer) at 37°C. After washing in phosphate buffer at room temperature, the samples were kept in 70% ethanol for chlorophyll destaining. The leaves were cleared as described in the 'Growth analysis' section and mounted in lactic acid. Images of GUS-stained plants were taken with the binocular microscope (MZ16; Leica) and Nikon camera.

RNA and quantitative RT-PCR

Total RNA was extracted from the first leaf pair with the RNeasy kit (Qiagen). Poly(dT) cDNA was prepared from 1 µg of total RNA with Superscript III reverse transcriptase (Invitrogen, Carlsbad, CA, USA) and analyzed on an LightCycler 480 apparatus (Roche Diagnostics, Basel, Switzerland) with the SYBR Green I Master kit (Roche Diagnostics, Basel, Switzerland) according to the manufacturer's instructions. Gene expression was quantified with a specific primer set (Table S1) designed with Beacon Designer 4.0 (Premier Biosoft International, Palo Alto, CA, USA). All individual reactions were performed in triplicate. Data were analyzed with qBase (Hellemans *et al.*, 2007). Expression levels were normalized to those of *26S PROTEASOME REGULATORY SUBUNIT S2 1A (PRS2)/REGULATORY PARTICLE NON-ATPASE1 (RPN1)*.

Immunoblot and protein quantification analysis

To extract proteins, the first leaf pair of plants at 8 or 12 DAS was frozen in liquid nitrogen, ground and homogenized in ice-cold extraction buffer (25 mM Tris–HCl, pH 7.6, 15 mM $MgCl_2$, 5 mM EGTA, 150 mM NaCl, 15 mM *p*-nitrophenyl phosphate, 60 mM β-glycerophosphate, 0.1% (v/v) Nonidet P-40, 0.1 mM sodium vanadate, 1 mM NaF, 1 mM dithiothreitol, 1 mM phenylmethylsulfonylfluoride, and 1 tablet per 10 ml of protease inhibitor cocktail (Roche, Basel, Switzerland)). The homogenate was centrifuged twice for 20 min at 20 800 ***g*** and 4° C and the protein concentration determined with QuickStartTM Bradford1X dye reagent (Bio-Rad Laboratories, Hercules, CA, USA). Approximately 45 µg of total proteins were mixed with 5X SDS sample buffer (250 mM Tris–HCl, pH 6.8, 50% glycerol, 5% SDS, 0,02% bromophenol blue and 0.5 M DTT), boiled for 10 min at 95°C, separated on a 15% (w/v) SDS-PAGE gel and further transferred to nitrocellulose membranes (Hybond-C super; GE-Healthcare, Little Chalfont, UK). Membranes were then stained with 0.1% (w/v) Ponceau solution and blocked overnight at 4°C. For immunodetection, monoclonal mouse anti-GFP antibody (Living Colors®; Clontech, Mountain View, CA, USA), polyclonal rabbit anti-KNOLLE antibody (gift from Gerd Jürgens) at 1 : 4000 dilution, and polyclonal rabbit anti-CDKA;1 PSTAIRE (Santa Cruz Biotechnology, Santa Cruz, CA, USA) at 1 : 2000 dilution were used as primary antibodies. A secondary anti-rabbit antibody (Amersham/GE Healthcare, Little Chalfont, UK) was used at 1 : 10 000 dilution. The proteins were detected by chemiluminescence reaction (Perkin-Elmer, Waltham, MA, USA). The images obtained were quantified using ImageJ software (Abràmoff *et al.*, 2004) by inverting the image and measuring the band of interest as the mean value of pixels per unit area. The set of bands were compared with corresponding nonspecific bands in order to subtract the background. Finally, the relative values of the signal were calculated as compared with the control sample. The number of biological repetitions for each experiment is indicated in each legend and the average value of the significant fold-change is presented below the representative blot.

Kinase assay

$P10^{CKS1At}$ was purified from an overproducing *Escherichia coli* strain and linked to CNBr-Sepharose 4B (GE-Healthcare, Little Chalfont, UK) according to Azzi *et al.* (1994). The beads were washed three times with homogenization buffer (HB) containing 25 mM Tris–HCl (pH 7.6), 60 mM β-glycerophosphate, 15 mM nitrophenyl phosphate, 15 mM EGTA (pH 8), 15 mM $MgCl_2$, 85 mM NaCl, 1 mM dithiothreitol, 0.1 mM vanadate, 1 mM NaF, 0.1 mM benzamidine, 1 mM phenylmethylsulfonylfluoride, 0.1% NP-40, and 1 tablet per 10 ml protease inhibitor cocktail (Roche, Basel, Switzerland). Protein extracts were prepared from the first leaf pair of the Col-0 wild type and *cpd* mutant in HB. In a total volume of 200 µl of HB, 350 µg of protein extract was loaded on 50 µl of 50% (v/v) $p10^{CKS1At}$-Sepharose beads and incubated on a rotating wheel for 2 h at 4°C. After brief centrifugation at 110 ***g*** and removal of the supernatant, the beads were carefully washed three times with bead buffer containing 50 mM Tris–HCl (pH 7.5), 5 mM NaF, 250 mM NaCl, 5 mM EGTA, 5 mM EDTA, 0.1% NP-40, 0.1 mM

benzamidine, 0.1 mM vanadate and 1 tablet per 10 ml protease inhibitor cocktail (Roche, Basel, Switzerland). The beads were washed once with kinase buffer (50 mM Tris–HCl (pH 7.8), 15 mM $MgCl_2$, 5 mM EGTA and 2 mM dithiothreitol), and the supernatant was removed carefully. The histone H1 kinase reactions were initiated by resuspending the pellets of $p10^{CKS1At}$-Sepharose beads in 35 µl of the reaction mixture containing 5 µCi [γ-^{33}P] ATP (3000 Ci mmol^{-1}), 0.5 mg ml^{-1} histone H1, 50 mM Tris–HCl (pH 7.8), 15 mM $MgCl_2$, 5 mM EGTA, 1 mM dithiothreitol, 60 µg ml^{-1} cAmp-dependent kinase inhibitor and 10 µM ATP. After 20 min of incubation at 30°C, the kinase reactions were stopped by the addition of 10X SDS/PAGE loading buffer. Aliquots were boiled, loaded on a 12% (w/v) acrylamide gel, and stained using Coomassie blue. The gel was dried overnight and incorporation of [γ-^{33}P] ATP into histone H1 was quantified with a PhosphorImager (Molecular Dynamics, Sunnyvale, CA, USA).

Statistical analysis

P values were calculated using a two-tailed Student's *t* -test and Excel software.

Results

BRs regulate leaf growth by promoting cell expansion, proliferation and differentiation

To understand how BRs regulate leaf growth, we compared leaves of wild-type plants with those of the BR loss-of-function mutant *cpd* which is deficient in a gene encoding a key enzyme, cytochrome P450 (CYP90), in the BR biosynthesis pathway (Szekeres *et al.*, 1996). The decreased BR levels in the *cpd* mutant resulted in fewer and significantly smaller, round-shaped leaves, as seen in leaf series of *in vitro* grown plants at 21 DAS (Fig. 1a). To gain insight into the cellular and developmental basis of this phenotype, the abaxial epidermis and palisade mesophyll of the first true leaf pair of the *cpd* mutant were analyzed. As under *in vitro* conditions the growth of those leaves is subdivided into three developmental phases, samples were collected at 8 DAS, corresponding to active cell proliferation, 12 and 16 DAS, corresponding to cell expansion, and 21 DAS, when both cell division and cell expansion have ceased (De Veylder *et al.*, 2001; Beemster *et al.*, 2005). At 21 DAS, the area of the *cpd* leaf blade showed a 70% reduction when compared with the wild type, which

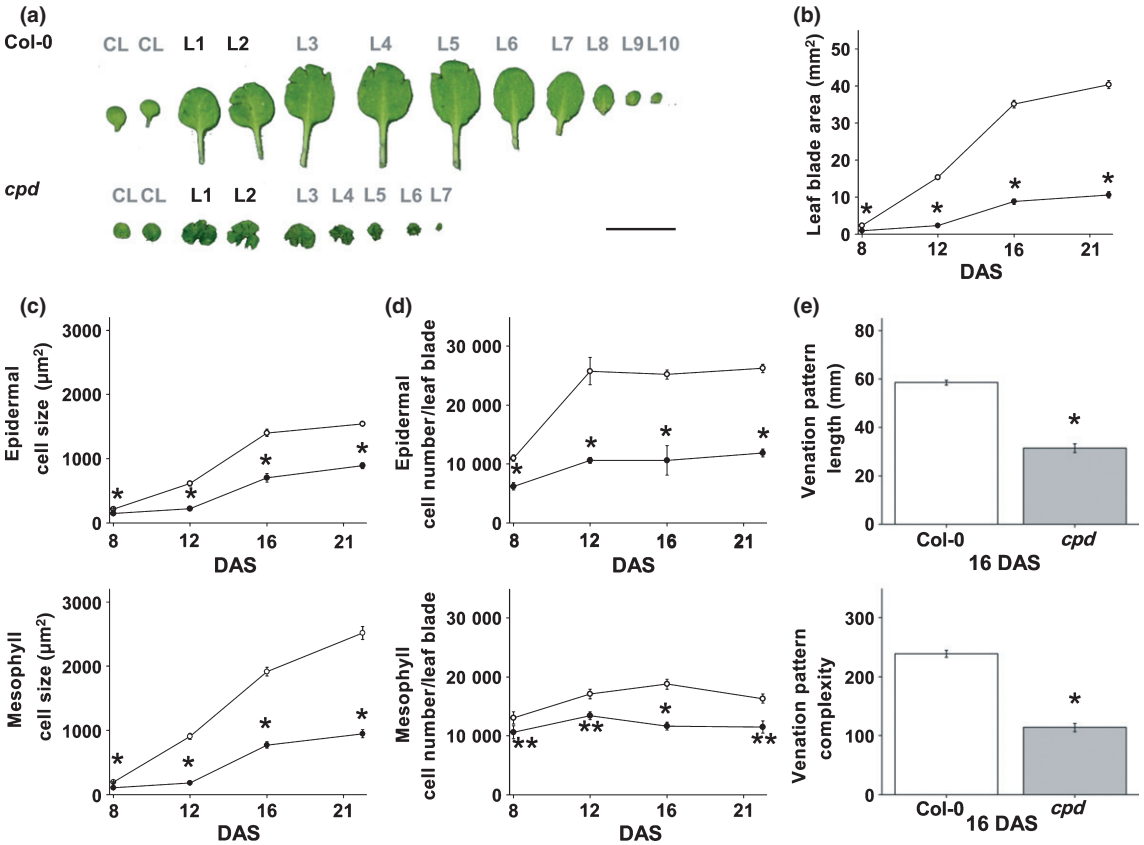

Fig. 1 Brassinosteroids (BRs) promote leaf growth in Arabidopsis. (a) Leaf series for the wild type (Col-0) and the BR-deficient mutant *constitutive photomorphogenesis and dwarfism* (*cpd*) at 21 d after sowing (DAS). CL, cotyledon; L, leaf; L1 and L2 (highlighted in black) were used for analyses. Bar, 1 cm. (b) Leaf area of Col-0 and *cpd* plants. (c) Cell size in the epidermis and mesophyll of Col-0 and *cpd* leaves. (d) Cell number in the epidermis and mesophyll of Col-0 and *cpd* leaves. (e) Venation pattern length and complexity in Col-0 and *cpd* leaves. Error bars indicate SE ($n > 10$). *P* value (*t*-test), * < 0.001 and ** < 0.05, relative to the wild type. *n*, number of leaves analyzed.

correlated with a significant decrease in both cell size and cell number in the epidermis and mesophyll (Fig. 1a–d). Interestingly, while the cell size was more reduced in the mesophyll, the cell number was more affected in the epidermis. The observed defects in epidermal cell expansion in the *cpd* mutant correlated with a less complex shape of the pavement cells, demonstrated by the higher circularity value (Andriankaja *et al.*, 2012) than that of the wild type (Fig. S1a,b).

To study the effect of BRs on leaf differentiation, we analyzed the leaf vasculature in the *cpd* mutant using parameters that quantitatively describe the leaf venation pattern (Dhondt *et al.*, 2012). When compared with the wild type, the leaves of the *cpd* mutant displayed a reduction in venation pattern length, number of areolas and branching end points, which resulted in an overall reduced venation pattern complexity (Figs 1e, S1c,d). Taken together, the described phenotypes highlight a role for BRs in leaf growth through promoting cell expansion, proliferation and differentiation, thus affecting the final size of the leaf.

BRs balance cell proliferation and expansion in the leaf

We next aimed to clarify whether the observed leaf phenotypes in the *cpd* mutant are attributable to disturbed coordination between cell division and expansion during leaf growth. Therefore, the cell division rate (De Veylder *et al.*, 2001; Achard *et al.*, 2009) was determined in the abaxial leaf epidermis of the *cpd* mutant and the wild type (Fig. S2a). Because of the dwarf nature of *cpd*, the earliest time-point examined was 8 DAS. The kinematic analysis showed that at this stage the cell division rate was lower in *cpd* than in the wild type, but between 10 and 14 DAS, when the transition from proliferation to expansion occurred, it declined more slowly in the mutant, indicating a delayed exit from cell proliferation. The average cell cycle duration (Fiorani & Beemster, 2006) in the whole leaf at 8 DAS was higher in *cpd* than in the wild type, being 31 and 25 h, respectively. Ploidy levels were measured at time intervals corresponding to the kinematic analysis and no significant changes were observed when compared with the wild type (Fig. S2b). We conclude that

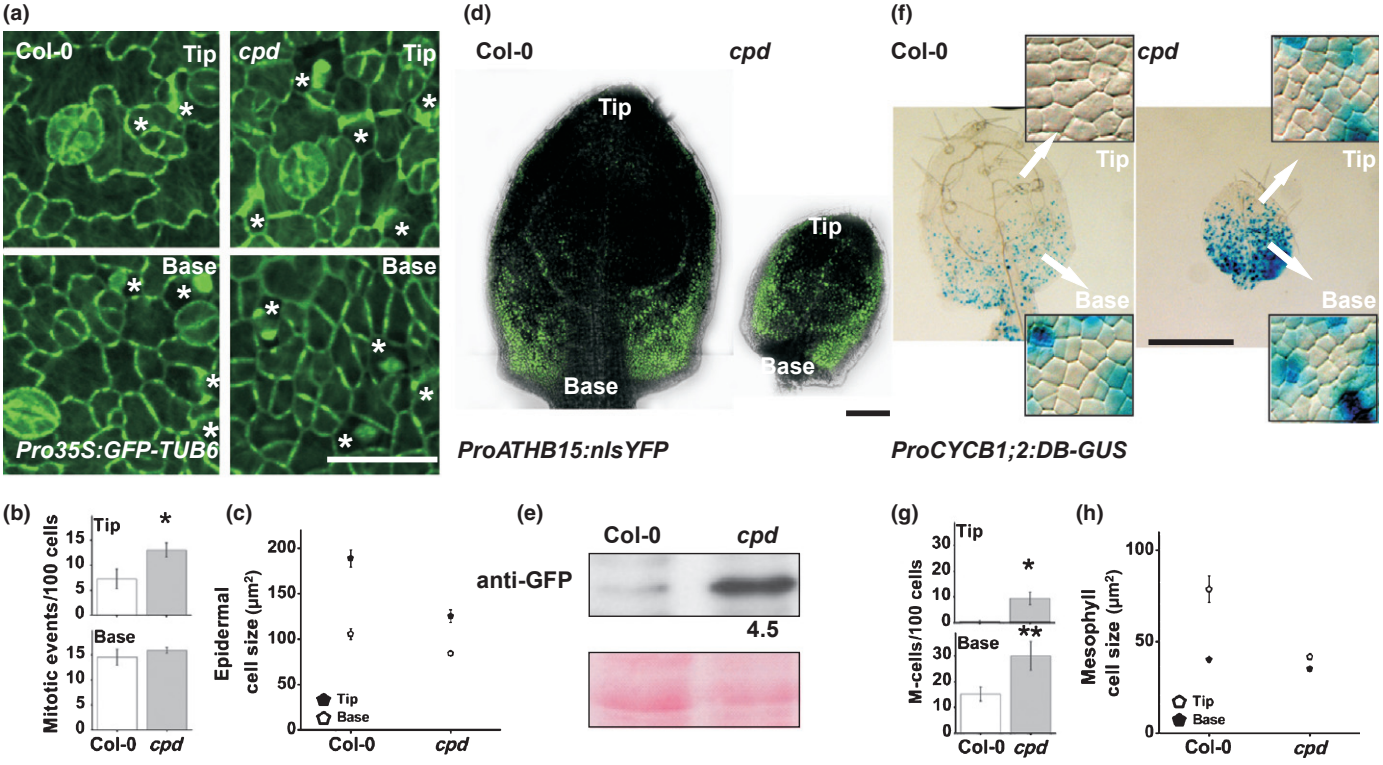

Fig. 2 Brassinosteroids (BRs) regulate cell proliferation, expansion and differentiation in the Arabidopsis leaf. (a) Expression of the *Pro35S:GFP-TUB6* marker in the epidermis of Col-0 and *constitutive photomorphogenesis and dwarfism* (*cpd*) leaves at 7 d after sowing (DAS). Insets from the leaf tip and base are shown. Asterisks indicate mitotic events. Bar, 0.1 mm. (b) Number of mitotic events per 100 epidermal cells in the leaf tip and base of Col-0 and *cpd* leaves carrying the *Pro35S:GFP-TUB6* marker at 7 DAS. Error bars indicate SE ($n > 10$). *P* value (*t*-test), * < 0.05, relative to the wild type. (c) Epidermal cell size in the leaf tip and base of Col-0 and *cpd* leaves carrying the *Pro35S:GFP-TUB6* marker at 7 DAS. Error bars indicate SE ($n > 10$). (d) Confocal images of Col-0 and *cpd* leaves at 7 DAS expressing *ProATHB15:nlsYFP*. Bar, 0.1 mm. (e) Immunodetection of YFP with anti-GFP antibody in protein extracts from Col-0 and *cpd* leaves expressing *ProATHB15:nlsYFP* at 8 DAS. Numbers indicate the estimated fold-change increase relative to Col-0 control, which is 1 ($n = 1$). Ponceau staining was used as a loading control. (f) Expression of *ProCYCB1;2:DB-GUS* in Col-0 and *cpd* leaves at 8 DAS. Insets represent mesophyll cells at the leaf tip and base. Bar, 0.5 mm. (g) Number of M cells per 100 mesophyll cells in the tip and base of Col-0 and *cpd* leaves carrying *ProCYCB1;2:DB-GUS* at 8 DAS. Error bars indicate SE ($n > 10$). *P* value (*t*-test), * < 0.005 and ** < 0.05 relative to the wild type. (h) Mesophyll cell size in the leaf tip and base of Col-0 and *cpd* leaves carrying *ProCYCB1;2: DB-GUS* at 8 DAS. Error bars indicate SE ($n > 10$). *n*, number of leaves analyzed, and in the case of the immunoblot – number of biological repetitions.

the reduced cell number in the epidermis of the *cpd* mutant is caused by a slower progression through the cell cycle and a delayed exit from cell division.

We further explored how BR deficiency affects the spatial coordination between cell division and cell expansion in the leaf at early developmental stages, namely 7 and 8 DAS. The cell division activity in the leaf abaxial epidermis was fine-mapped using the tubulin marker *Pro35S:GFP-TUB6* (Snustad *et al.*, 1992; Nakamura *et al.*, 2004), which visualizes the mitotic spindles denoting mitotic events (Fig. 2a). The epidermal cell size and the frequency of mitotic events were measured at the leaf base (at 25% of the leaf blade length) and at the leaf tip (at 75% of the leaf blade length) at 7 DAS. When compared with the wild type, the fraction of mitotic cells at the leaf tip of the *cpd* mutant was higher (Fig. 2b) and correlated with a reduction in epidermal cell size (Fig. 2c) and number (Fig. 1d). Also, the percentage of mitotic events per total epidermal cell number was slightly, but significantly, increased in *cpd* leaves at 7 DAS (Fig. S3a). These data indicate that in *cpd* epidermal cells reside in the M phase for longer.

We next investigated whether leaf differentiation is delayed in *cpd* by analyzing the expression of the transcription factor *ATHB15* which negatively regulates vascular cell differentiation (Ohashi-Ito & Fukuda, 2003). At 7 DAS, the *ProATHB15:nlsYFP* fluorescence was observed in the differentiating vascular bundles of the wild-type leaf base, while in *cpd* leaves the expression was observed in a broader area along the leaf length (Fig. 2d), suggesting a delay in differentiation. The prolonged *ProATHB15:nlsYFP* activity in *cpd* leaves correlated with more than a fourfold increase in the accumulation of YFP protein in whole *cpd* leaf extracts (Fig. 2e). Thus, our results support a role for BRs in controlling the exit from mitosis in the leaf.

BRs control the exit from mitosis

To further unravel the nature of the M-phase defects in *cpd* leaves, we analyzed the expression of the B-type cyclin marker *ProCYCB1;2:DB-GUS*, which accumulates during mitosis and is degraded at anaphase as a result of the presence of a destruction box (DB; Colón-Carmona *et al.*, 1999; Schnittger *et al.*, 2002), in the leaf mesophyll of *cpd* and wild-type plants at 8 DAS (Fig. 2f). *cpd* displayed an increase in the number of cells labeled with *CYCB1;2:DB-GUS*, both at the base and at the tip of the leaf, whereas in the wild type, *CYCB1;2:DB-GUS*-labeled cells were confined to the leaf base (Figs 2f,g, S3b). In accordance with this finding, the transition toward cell expansion was delayed in the mesophyll cells of *cpd* (Fig. 2h). To understand why *ProCYCB1;2:DB-GUS* accumulates in *cpd*, we measured the *CYCB1;2* and *GUS* transcript levels in leaves of the same lines (Figs 3a, S3c). Although a slight increase in *GUS* transcript levels was observed in *cpd* (Fig. S3c), the endogenous B-type cyclin transcripts were slightly reduced in this mutant *cpd* (Fig. 3a). Similarly, the transcription of the M phase-expressed syntaxin *KNOLLE* (Völker *et al.*, 2001) was not increased (Fig. 3a), whereas a significant accumulation of its protein was detected in *cpd* at 8 DAS by immunoblot analysis (Fig. 3b). Because

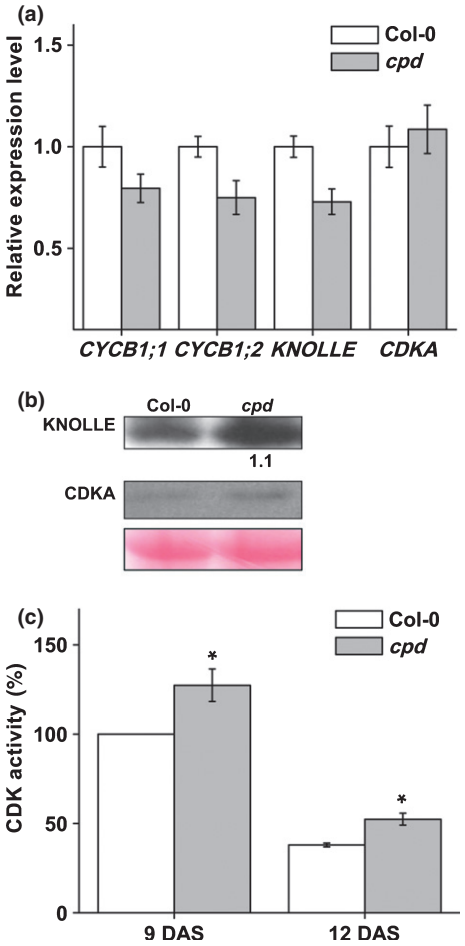

Fig. 3 Brassinosteroids (BRs) control mitosis in Arabidopsis. (a) Relative mRNA expression levels of *CYCB1;1*, *CYCB1;2*, *KNOLLE*, and *CDKA;1* in Col-0 and *constitutive photomorphogenesis and dwarfism* (*cpd*) leaves at 8 d after sowing (DAS). Error bars indicate SD ($n = 3$). (b) A representative image of immunodetection of KNOLLE and CDKA;1 with antibodies against KNOLLE and CDKA;1 in protein extracts from Col-0 and *cpd* leaves at 8 DAS. Numbers indicate an average value of the estimated fold-increase of protein level in *cpd* relative to the Col-0 control, which is 1 ($n = 3$). Ponceau staining is shown as a loading control. (c) CYCLIN-DEPENDENT KINASE (CDK) activity assay in Col-0 and *cpd* leaves at 9 and 12 DAS. Error bars indicate SD ($n = 2$). *P* value (*t*-test), * < 0.05, relative to the wild type. *n*, number of biological repetitions.

CYCLIN-DEPENDENT KINASE (CDK) activity is known to peak during mitosis, we tested the total CDK activity in leaves. Notably, 20% higher CDK activity was observed in *cpd* compared with wild-type leaves (Fig. 3c). The *CDKA;1* transcription and CDKA;1 protein levels were not changed (Fig. 3a,b).

To investigate whether an increase in mitotic activity is sufficient to reverse the BR-deficient leaf phenotype, a transgenic line overexpressing *CYCD3;1* (*CYCD3;1*^{OE}) (Dewitte *et al.*, 2003) was introduced into the *cpd* mutant (Fig. 4a,b) and analyzed at 12 DAS. Overexpression of *CYCD3;1* restored the mitotic activity in *cpd*, as leaves of *cpd*;*CYCD3;1*^{OE} plants contained numerous small cells both in the epidermis and in the mesophyll, similarly to the *CYCD3;1*^{OE} line (Fig. 4c,d). As expected for dividing tissues, the protein level of KNOLLE was increased (Fig.

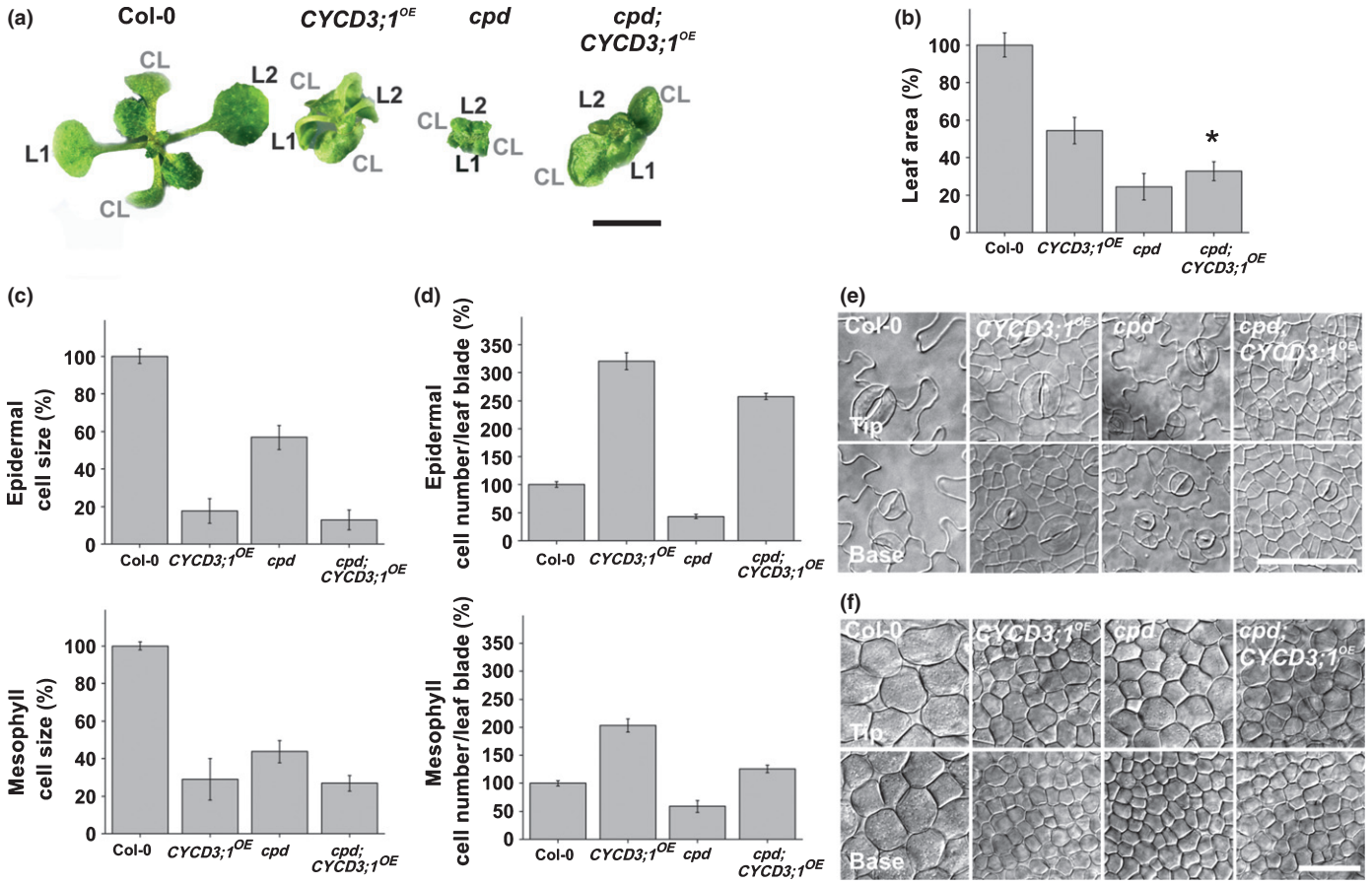

Fig. 4 Ectopic cell division restores the cell number but not the cell size in leaves of Arabidopsis *constitutive photomorphogenesis and dwarfism* (*cpd*) mutant. (a) Rosettes of Col-0, *CYCD3;1*^{OE}, *cpd*, and *cpd;CYCD3;1*^{OE} plants at 12 d after sowing (DAS). CL, cotyledon; L, leaf; L1 and L2, the first leaf pair, are highlighted in black. Bar, 0.5 cm. (b) Leaf blade area of Col-0, *CYCD3;1*^{OE}, *cpd*, and *cpd;CYCD3;1*^{OE} plants at 12 DAS. Error bars indicate SE ($n > 10$). *P* value (*t*-test), * < 0.001, relative to *cpd*. (c) Epidermal and mesophyll cell size of Col-0, *CYCD3;1*^{OE}, *cpd*, and *cpd;CYCD3;1*^{OE} leaves at 12 DAS. Error bars indicate SE ($n > 10$). (d) Epidermal and mesophyll cell number of Col-0, *CYCD3;1*^{OE}, *cpd*, and *cpd;CYCD3;1*^{OE} leaves at 12 DAS. Error bars indicate SE ($n > 10$). (e) DIC microscopic images of the epidermis (at the leaf tip and base) of Col-0, *CYCD3;1*^{OE}, *cpd*, and *cpd;CYCD3;1*^{OE} leaves at 12 DAS. Bar, 0.05 mm. (f) DIC microscopic images of the mesophyll (at the leaf tip and base) of Col-0, *CYCD3;1*^{OE}, *cpd*, and *cpd;CYCD3;1*^{OE} leaves at 12 DAS. Bar, 0.05 mm. *n*, number of leaves analyzed.

S4). Although the high *CYCD3;1* expression in *cpd* was able to restore the cell number deficit, the cells remained small at both the base and the tip of the leaf, demonstrating a defect in the transition toward expansion along the leaf length (Fig. 4e,f). These results show that a complete restoration of the BR-deficient leaf phenotypes requires BR-mediated cell expansion and differentiation.

Exogenous application of BRs triggers differentiation in the leaf

It was previously shown that the dwarf leaf phenotype of the *cpd* mutant is restored to the wild-type size by exogenous application of the most active BR, brassinoslide (BL; Szekeres *et al.*, 1996). We used this experimental system as a tool to investigate whether the cell expansion and division defects in the *cpd* mutant are completely restored by the BL treatment. For this, *cpd* plants at 8 DAS were transferred to medium supplemented with 100 nM BL and analyzed after 24–96 h (Fig. 5a). Forty-eight hours of BL treatment increased the size of the *cpd* leaf blade by 60%, whereas a longer application of BL had a mostly inhibitory effect on leaf growth. Interestingly, the enlargement of the leaf blade at 48 h was a result of induced cell expansion in both the epidermis and the mesophyll (Fig. 5b). Notably, a slight, but significant, increase in cell number was found only in the epidermis (Fig. 5c). BL also promoted cell expansion along the leaf in the epidermis and mesophyll (Fig. 5d), which correlated with a reduction of the percentage of mitotic cells labeled with *CYCB1;2:DB* in the mesophyll (Fig. 5e), as well as a marked decrease in the abundance of total KNOLLE and CDKA;1 proteins (Fig. 5f). Our data show that the exogenously applied BL triggers mitotic cell cycle exit and differentiation in the leaf. This observation was further supported by the cellular analysis of leaves of plants overexpressing a key BR biosynthetic enzyme, DWARF4 (*DWF4*^{OE}), and thus presumably accumulating BRs (Choe *et al.*, 2001; Wang *et al.*, 2001). At 12 DAS, the size of both epidermal and mesophyll cells was increased compared with the wild type, while the total cell number was unaffected in the

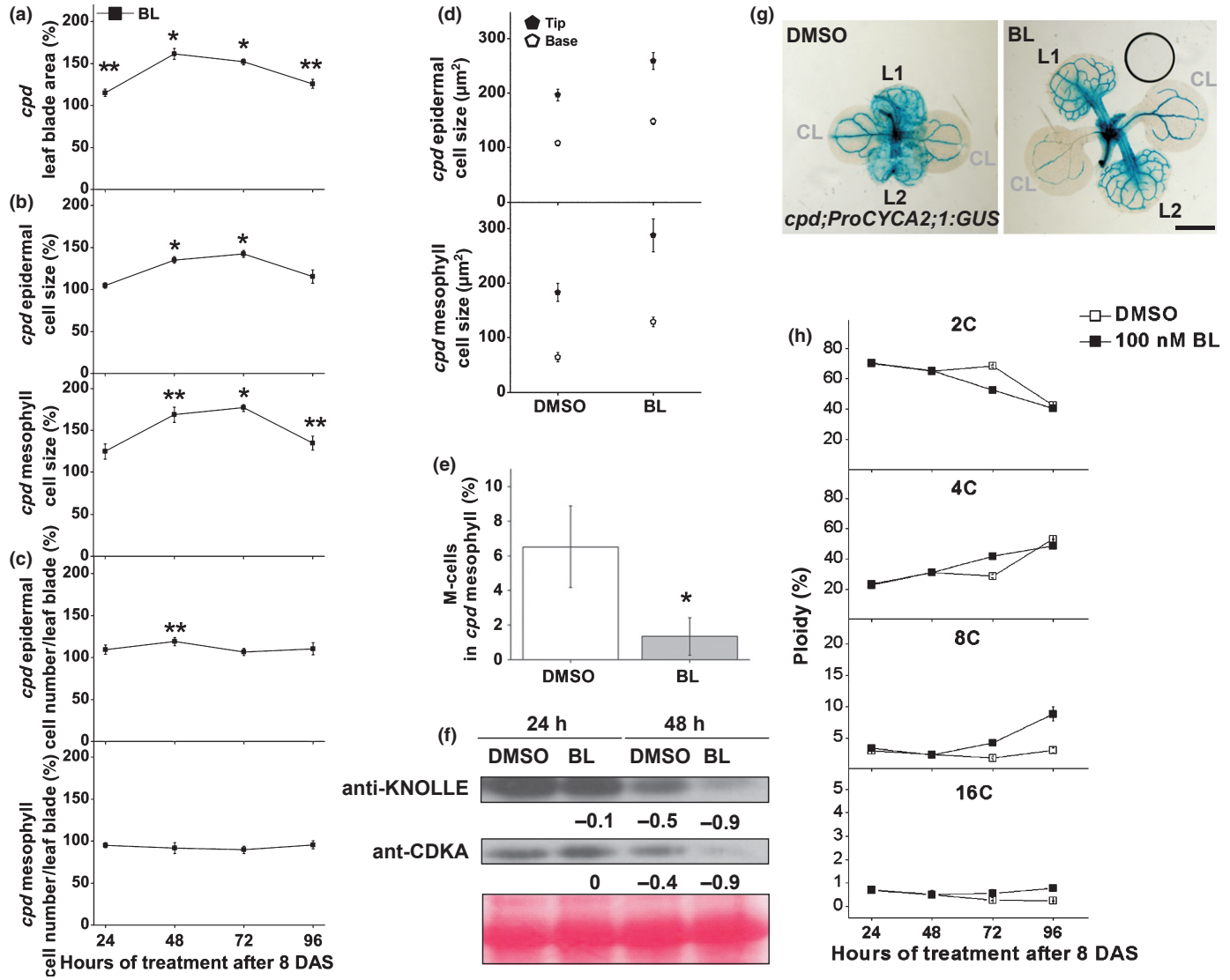

Fig. 5 Exogenous brassinosteroids (BRs) rescue the leaf phenotypes of the Arabidopsis *constitutive photomorphogenesis and dwarfism (cpd)* mutant. (a) Leaf blade area. (b) Cell size. (c) Cell numbers of leaf epidermis and mesophyll of *cpd* plants treated at 8 d after sowing (DAS) with DMSO mock or 100 nM BL. The DMSO-treated *cpd* plants are used as a relative control equal to 100%. Error bars indicate SE ($n > 10$). *P* value (*t*-test), * < 0.001 and ** < 0.05, relative to DMSO-treated *cpd*. (d) Epidermal and mesophyll cell size in the tip and base of leaves of *cpd* plants treated at 8 DAS with DMSO or 100 nM BL for 48 h. Error bars indicate SE ($n > 10$). *P* value (*t*-test), tip < 0.05 and base < 0.001, relative to DMSO-treated *cpd*. (e) Percentage of M cells per total mesophyll cell number of leaves of *cpd* plants carrying the *ProCYCB1;2:DB-GUS* marker and treated at 8 DAS with DMSO or 100 nM BL for 48 h. Error bars indicate SE ($n > 10$). *P* value (*t*-test), * < 0.05, relative to DMSO-treated *cpd*. (f) Immunodetection of KNOLLE and CDKA;1 in protein extracts from leaves of *cpd* plants treated at 8 DAS with DMSO or 100 nM BL for 24 and 48 h. Numbers indicate estimated fold-change of protein level relative to the respective control (i.e. *cpd* plants treated at 8 DAS with DMSO for 24 h). Ponceau staining was used as a loading control ($n = 1$). (g) Expression of *ProCYCA2;1:GUS* in leaves of *cpd* plants treated at 8 DAS with DMSO or 100 nM BL for 48 h. CL, cotyledon; L, leaf; L1 and L2, the first leaf pair, highlighted in black. Bar, 1 mm. (h) Ploidy level in leaves of *cpd* plants treated at 8 DAS with DMSO or 100 nM BL. Error bars indicate SE ($n > 10$) of two biological repeats. *n*, number of leaves analyzed, and in the case of the immunoblot – number of biological repetitions.

epidermis and slightly, but significantly, reduced in the mesophyll (Fig. S5a–c).

Application of BL also enhanced the vascular differentiation of the leaf in *cpd* after treatment with BL for 48 h, as seen from the expression of three vascular markers, that is, the A2-type cyclin *ProCYCA2;1:GUS* (Fig. 5g; Vanneste *et al.*, 2011), the auxin efflux carrier *ProPIN1:GUS* (Friml *et al.*, 2003), and the auxin reporter *ProDR5:GUS* (Ulmasov *et al.*, 1997; Fig. S5e). During early Arabidopsis leaf development, the *CYCA2;1* and *PIN-FORMED1 (PIN1)* markers are expressed in relatively broad regions containing proliferating cells. Later their expression becomes restricted to the provascular strands, which is indicative of leaf differentiation (Scarpella *et al.*, 2006; Wenzel *et al.*, 2007). In *cpd* leaves at 9 DAS, the diffused *GUS* expression pattern persisted longer than in the wild type (Fig. S5d), whereas the application of BL accelerated the transition to bundle-specific expression (Fig. S5e). The delayed vascular differentiation caused by BR deficiency correlated with a decrease in auxin responses, as

demonstrated by the reduced *DR5:GUS* expression in *cpd* leaves, while BL application had the opposite effect (Fig. S5d,e).

The increase in epidermal and mesophyll cell size, the reduced protein level of cell division proteins, and the enhanced vascular differentiation in *cpd* leaves treated with BL all suggest that addition of BRs stimulates the onset of differentiation. As the exit from the cell cycle is followed by an endoreduplication cycle (De Veylder *et al.*, 2011), we measured the DNA content in leaf samples treated with BL. As predicted, application of BL for 72 h resulted in an accelerated mitotic exit, as demonstrated by the increased fraction of 8C cells, marking endoreduplication (Fig. 5h).

BRI1-dependent signaling fine-tunes leaf growth in Arabidopsis

To explore the role of BR signaling in leaf development, we analyzed the respective gain- and loss-of-function Arabidopsis BR signaling mutants $BRI1^{OE}$ and *bri1-116* (Friedrichsen *et al.*, 2000). Plants were grown in soil and the leaf cell size and cell number were analyzed at 8, 12, 16, and 21 DAS (Fig. 6a–c). When compared with the wild type, *bri1-116* leaves at 21 DAS had smaller and fewer cells in both the epidermis and the mesophyll (Fig. 6b,c), which correlated with the 80% reduction in the leaf blade area (Fig. 6a). By contrast, the leaves of the $BRI1^{OE}$ line contained a higher cell number and slightly larger cells in both the epidermis and the mesophyll (Fig. 6b,c), resulting in an 80% increase in the leaf blade area when compared with the wild type at 21 DAS (Fig. 6a). Similarly to *cpd*, the mitotic *ProCYCB1;2:GUS* accumulated in *bri1-116* when the DB motif was present (Fig. 6d). Consistent with the observed increase in cell number in the $BRI1^{OE}$ leaves, the expression of *ProCYCB1;2:DB-GUS* and *ProCYCB1;1:DB-GUS* was also increased (Figs 6d, S6a). Correspondingly, the percentage of mitotic cells in both *bri1-116* and $BRI1^{OE}$ leaves was higher than in wild-type leaves (Fig. 6e). As in *cpd*, the *bri1-116* leaves

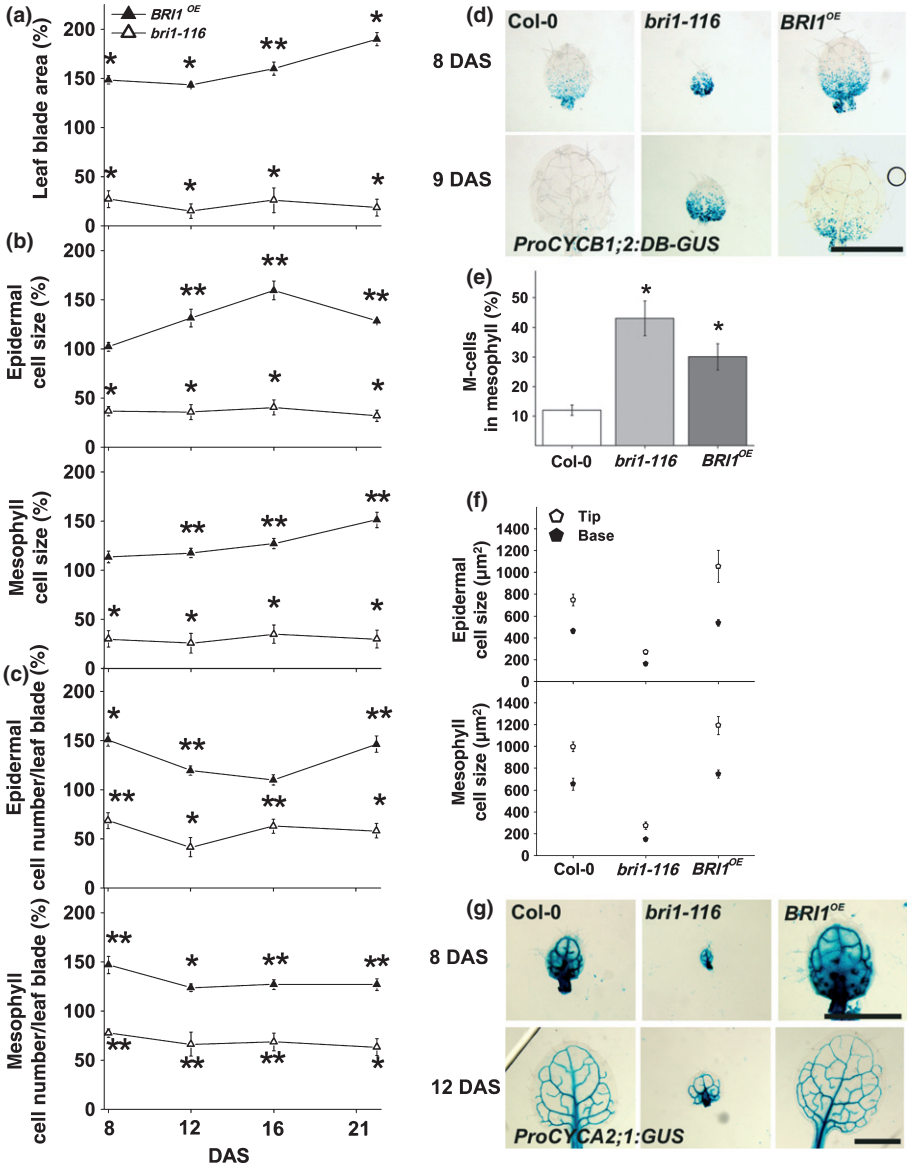

Fig. 6 Brassinosteroid (BR) signaling is required to fine-tune leaf growth in Arabidopsis. (a) Leaf area. (b) Epidermal and mesophyll cell size. (c) Epidermal and mesophyll cell number of Col-0, *bri1-116* and $BRI1^{OE}$ plants at 8, 12, 16, and 21 d after sowing (DAS). Col-0 plants were used as a relative control equal to 100%. Error bars indicate SE ($n > 10$). *P* value (*t*-test), * < 0.001 and ** < 0.05, relative to the wild type. (d) Expression of *ProCYCB1;2:DB-GUS* in leaves of Col-0, *bri1-116* and $BRI1^{OE}$ plants. Bar, 1 mm. (e) Number of M cells per total mesophyll cell number in the tip and base of Col-0, *bri1-116* and $BRI1^{OE}$ leaves carrying the *ProCYCB1;2:DB-GUS* marker at 8 DAS. Error bars indicate SE ($n > 10$). *P* value (*t*-test), * < 0.005, relative to the wild type. (f) Epidermal and mesophyll cell size at the tip and base of Col-0, *bri1-116* and $BRI1^{OE}$ leaves at 12 DAS. Error bars indicate SE ($n > 10$). *P* value (*t*-test), tip < 0.05 (for *bri1-116* and $BRI1^{OE}$), base < 0.005 (for *bri1-116*), relative to the wild type (Col-0). (g) Expression of *ProCYCA2;1:GUS* in leaves of Col-0, *bri1-116* and $BRI1^{OE}$ plants. Bar, 1 mm. *n*, number of leaves analyzed.

displayed a delay in both cell elongation and vascular development along the leaf (Fig. 6f,g). By contrast, compared with the wild type, at 12 DAS the *BRI1*^{OE} leaves were characterized by accelerated cell expansion along the leaf blade (Fig. 6f), as well as vasculature development defined by the faster decline in the expression of the provascular markers *CYCA2;1:GUS* and *PIN1:GUS* at the leaf tip (Figs 6g, S6b). Notably, the expression of *DR5:GUS* in the *BRI1*^{OE} leaves did not increase (Fig. S6c), which differed from wild-type leaves treated with BL (Bao *et al.*, 2004). We conclude that the enhanced BR signaling in *BRI1*^{OE} plants favors optimal BR responses for stimulating epidermal and mesophyll cell division and cell expansion, as well as vasculature development in the leaf.

Discussion

BR synthesis and BRI1-mediated signaling differentially affect cell division and expansion in the leaf

The final size and shape of the leaf are defined by the genetic program and environmental stimuli (Skirycz & Inzé, 2010; Gonzalez *et al.*, 2012). Our study revealed that the plant hormones BRs promote leaf growth by affecting cell proliferation and expansion and this effect is strongly dependent on BR levels and BRI1-mediated signaling. As a general tendency, a deficiency in either BR biosynthesis or signaling caused smaller leaves with a decreased number and size of epidermal and mesophyll cells. Conversely, plants displaying constitutive BR responses including BR biosynthesis and signaling gain-of-function mutants had larger leaves. Whereas the larger leaf size in plants overproducing the BRI1 receptor (*BRI1*^{OE}) in its native domain was attributable to an increase mainly in cell number, the larger leaves of plants with enhanced BR biosynthesis (*DWF4*^{OE}) were solely caused by an increase in cell size. Similarly, the rescue of the small *cpd* leaves by exogenous application of BRs was a result more of cell expansion than division. Previous reports also showed that the growth promotion in leaves associated with BR signaling, in plants overexpressing either the *BRI1* receptor or its phosphorylation variant *BRI1 (Y831F)*, was coupled with an increase in cell number (Gonzalez *et al.*, 2010; Oh *et al.*, 2011). By contrast, the gain-of-function mutant of the *BREVIS RADIX* gene encoding a putative transcription factor with an impact on BR biosynthesis, resulting in increased BR levels, showed a promoting effect on cell expansion in the same organ (Beuchat *et al.*, 2010). Based on these observations, we conclude that manipulation of BR signaling affects cell division, whereas manipulation of BR levels affects cell expansion. We speculate that the different cellular phenotypes observed in BR signaling and biosynthesis mutants are related to differences in the ratio of receptor (BRI1)/ligand (BL) concentrations, which consequently trigger downstream BR responses with distinctive outputs. Similarly, in Arabidopsis roots optimal BR signaling is required to promote meristematic divisions, whereas enhanced BR signaling caused by a gain-of-function mutation in BES1 (*bes1-D*) induced early differentiation (González-García *et al.*, 2011). It was recently postulated that the density of the BRI1 receptor in different cell types of the Arabidopsis root is an important element in BRI1-mediated signaling, as it determines the cell sensitivity to BRs in different tissues (González-García *et al.*, 2011; Hacham *et al.*, 2011; Van Esse *et al.*, 2011). It will be of interest to further investigate whether a similar scenario is applicable to the leaf.

The mature vegetative leaf of Arabidopsis consists of an outer epidermis, internal mesophyll and vasculature (Tsukaya, 2005). Earlier reports determined that BRI1 activity in the epidermis only is required for the growth of Arabidopsis leaves, although *BRI1* expression was detected in almost all cells (Savaldi-Goldstein *et al.*, 2007). Notably, we observed differences in the BR effect between the epidermis and the mesophyll in the leaves of BR loss- and gain-of-function mutants. Whereas cell division was affected more in the epidermis, the effect on cell size was more pronounced in the mesophyll. The molecular basis of these different responses remains unknown. It has been shown that the epidermis and palisade mesophyll in Arabidopsis leaves display a similar gradient in division pattern and they have a similar frequency of cell division (Andriankaja *et al.*, 2012). Thus, while the basic mechanism of cell division is presumably common to both tissue layers, tissue layer-specific upstream signaling regulation, possibly via BR biosynthesis, catabolism, and signaling, might balance the growth behavior of each tissue within the leaf. In addition to cell size and cell number, the reduced leaf size of the *cpd* mutant was associated with a shorter venation pattern length and an overall reduced complexity, whereas increased BR signaling or application of BRs accelerated vascular differentiation in the leaf.

BRs regulate the boundary between cell division and expansion in the leaf

Mutants defective in BR biosynthesis or perception have characteristically small, round leaves (Kauschmann *et al.*, 1996; Szekeres *et al.*, 1996; Azpiroz *et al.*, 1998), suggesting that they stopped growing along the leaf length. In agreement with this conclusion, exogenous application of BRs recovered the size and shape of the *det2* mutant leaves by a stimulatory effect on cell division and cell elongation, predominately in the longitudinal direction (Nakaya *et al.*, 2002). It was previously shown that leaf growth in Arabidopsis involves the establishment of a basiplastic (apex to base) cell division gradient along the blade. Thus, proliferative cell divisions initially are observed throughout the leaf, but gradually become restricted to more basal portions of the leaf blade (Donnelly *et al.*, 1999). Recently, it was revealed that the boundary between cell division and expansion, called an arrest front, remains at a constant distance from the leaf blade base during early stages of leaf development (4–7 DAS) and later (7–8 DAS) moves to the leaf base and disappears (Kazama *et al.*, 2010; Andriankaja *et al.*, 2012). Indeed, in the *cpd* mutant this arrest front is retained longer than in the wild type, although our leaf staging might differ from that of Kazama *et al.* (2010) as a consequence of different growth conditions. However, because fewer cells were found in *cpd* leaves, we conclude that the longer maintenance of the arrest front in *cpd* is not a compensatory mechanism for cell expansion defects (Tsukaya, 2006; Bögre *et al.*, 2008) but is probably a result of impaired cell production

and differentiation. Further analysis will be essential to clarify the role of BRs in this process.

BRs control the exit from mitosis

Our study shows that BRs control the exit from mitosis. Even though the transcript levels of the mitotic marker genes *CYCB1;1, CYCB1;2* and *KNOLLE* were slightly reduced in the *cpd* leaves, supporting recent observations made in seedlings of the BR-insensitive mutant *bri1-116* (Hacham *et al.*, 2011), an accumulation of proteins of the same markers was detected. Thus, it appears that M-phase-specific cell cycle proteins fail to degrade in the loss-of-function BR mutants. The increased CDK activity in *cpd* leaves also supports mitotic defects related to anaphase promoting complex/cyclosome (APC/C)-mediated regulation. APC/C has been implicated in leaf development, as the constitutive overexpression of the APC/C subunit *APC10* in Arabidopsis enhanced leaf size as a result of enhanced rates of cell division and increased proteolysis of CYCB1;1 (Eloy *et al.*, 2011). Remarkably, post-mitotic cells might also require APC/C activity for differentiation (Marrocco *et al.*, 2009). Therefore, BRs might regulate division and/or differentiation through modulation of APC/C activity via an as yet unknown mechanism. A previous work linked the increase in CYCB1 protein levels with an aberrant function of the Arabidopsis separase, which is required at anaphase onset to separate the sister chromatids (Wu *et al.*, 2010). However, a BR function in separase activities including chromatin maintenance or DNA repair is not known. The CYCB1 accumulation as a consequence of stabilization in different backgrounds results in disturbed cortical microtubule organization (Weingartner *et al.*, 2004; Serralbo *et al.*, 2006; Pérez-Pérez *et al.*, 2008). Although the CYCB1 accumulation and the higher CDK activity in *cpd* leaves correlated with irregular epidermal cell shape reflecting cytoskeleton organization defects, it remains to be determined whether this is the case in BR loss-of-function mutants.

In conclusion, we demonstrate that BRs are essential for cell division, expansion and differentiation in the leaf. The balance between proliferation and differentiation in a temporal and spatial manner depends on BR levels and BRI1-mediated signaling. However, further analysis will be essential to clarify the exact molecular mechanisms.

Acknowledgements

We thank M. Szekeres, T. Hashimoto, T. Beeckman, G. Jürgens and N. Raikhel for providing materials; M-C. Baroso for technical assistance; G. Gudesblat, N. Irani, D. Van Damme, V. Vassileva, S. Vanneste, J. Kleine-Vehn, S. Naramoto and P. Marhavy for useful discussions and critical reading of the manuscript; and M. De Cock and A. Bleys for help in preparing the manuscript. This work was supported by the FP7 Marie-Curie Initial Training Network 'BRAVISSIMO' (PITN-GA-2008-215118; E.R. and A.C-D), the Belgian Science Policy (BELSPO) (M.K.Z.) and the Agency for Innovation by Science and Technology (IWT) (who awarded a postdoctoral fellowship to M.K.Z., a pre-doctoral fellowship to S.D. and a 'Strategisch Basisonderzoek' grant (no. 60839) to C.B.). A.C-D. receives funding through grants from the Spanish Ministry of Science and Innovation (BIO2008/00505).

References

Abràmoff MD, Magalhães PJ, Ram SJ. 2004. Image processing with ImageJ. *Biophotonics International* **11**: 36–42.

Achard P, Gusti A, Cheminant S, Alioua M, Dhondt S, Coppens F, Beemster GTS, Genschik P. 2009. Gibberellin signaling controls cell proliferation rate in *Arabidopsis*. *Current Biology* **19**: 1188–1193.

Andriankaja M, Dhondt S, De Bodt S, Vanhaeren H, Coppens F, De Milde L, Mühlenbock P, Skirycz A, Gonzalez N, Beemster GTS *et al.* 2012. Exit from proliferation during leaf development in *Arabidopsis thaliana*: a not-so-gradual process. *Developmental Cell* **22**: 64–78.

Azpiroz R, Wu Y, LoCascio JC, Feldmann KA. 1998. An Arabidopsis brassinosteroid-dependent mutant is blocked in cell elongation. *Plant Cell* **10**: 219–230.

Azzi L, Meijer L, Ostvold A-C, Lew J, Wang JH. 1994. Purification of a 15-kDa cdk4- and cdk5-binding protein. *Journal of Biological Chemistry* **269**: 13279–13288.

Bao F, Shen J, Brady SR, Muday GK, Asami T, Yang Z. 2004. Brassinosteroids interact with auxin to promote lateral root development in Arabidopsis. *Plant Physiology* **134**: 1624–1631.

Beemster GTS, De Veylder L, Vercruysse S, West G, Rombaut D, Van Hummelen P, Galichet A, Gruissem W, Inzé D, Vuylsteke M. 2005. Genome-wide analysis of gene expression profiles associated with cell cycle transitions in growing organs of Arabidopsis. *Plant Physiology* **138**: 734–743.

Beuchat J, Scacchi E, Tarkowska D, Ragni L, Strnad M, Hardtke CS. 2010. *BRX* promotes Arabidopsis shoot growth. *New Phytologist* **188**: 23–29.

Bögre L, Magyar Z, López-Juez E. 2008. New clues to organ size control in plants. *Genome Biology* **9**: 226.

Caño-Delgado A, Yin Y, Yu C, Vafeados D, Mora-García S, Cheng J-C, Nam KH, Li J, Chory J. 2004. BRL1 and BRL3 are novel brassinosteroid receptors that function in vascular differentiation in Arabidopsis. *Development* **131**: 5341–5351.

Cheon J, Park S-Y, Schulz B, Choe S. 2010. Arabidopsis brassinosteroid biosynthetic mutant *dwarf7-1* exhibits slower rates of cell division and shoot induction. *BMC Plant Biology* **10**: 270.

Choe S, Dilkes BP, Fujioka S, Takatsuto S, Sakurai A, Feldmann KA 1998. The *DWF4* gene of Arabidopsis encodes a cytochrome P450 that mediates multiple 22α-hydroxylation steps in brassinosteroid biosynthesis. *Plant Cell* **10**: 231–243.

Choe S, Dilkes BP, Gregory BD, Ross AS, Yuan H, Noguchi T, Fujioka S, Takatsuto S, Tanaka A, Yoshida S *et al.* 1999. The Arabidopsis *dwarf1* mutant is defective in the conversion of 24-methylenecholesterol to campesterol in brassinosteroid biosynthesis. *Plant Physiology* **119**: 897–907.

Choe S, Fujioka S, Noguchi T, Takatsuto S, Yoshida S, Feldmann KA. 2001. Overexpression of *DWARF4* in the brassinosteroid biosynthetic pathway results in increased vegetative growth and seed yield in Arabidopsis. *Plant Journal* **26**: 573–582.

Chory J, Nagpal P, Peto CA. 1991. Phenotypic and genetic analysis of *det2*, a new mutant that affects light-regulated seedling development in Arabidopsis. *Plant Cell* **3**: 445–459.

Clough SJ, Bent AF. 1998. Floral dip: a simplified method for *Agrobacterium*-mediated transformation of *Arabidopsis thaliana*. *Plant Journal* **16**: 735–743.

Clouse SD, Langford M, McMorris TC. 1996. A brassinosteroid-insensitive mutant in *Arabidopsis thaliana* exhibits multiple defects in growth and development. *Plant Physiology* **111**: 671–678.

Colón-Carmona A, You R, Haimovitch-Gal T, Doerner P. 1999. Spatio-temporal analysis of mitotic activity with a labile cyclin-GUS fusion protein. *Plant Journal* **20**: 503–508.

De Smet I, Vassileva V, De Rybel B, Levesque MP, Grunewald W, Van Damme D, Van Noorden G, Naudts M, Van Isterdael G, De Clercq R *et al.* 2008. Receptor-like kinase ACR4 restricts formative cell divisions in the Arabidopsis root. *Science* **322**: 594–597.

De Veylder L, Beeckman T, Beemster GTS, Krols L, Terras F, Landrieu I, Van Der Schueren E, Maes S, Naudts M, Inzé D. 2001. Functional analysis of cyclin-dependent kinase inhibitors of Arabidopsis. *Plant Cell* **13**: 1653–1667.

De Veylder L, Larkin JC, Schnittger A. 2011. Molecular control and function of endoreplication in development and physiology. *Trends in Plant Science* **16**: 624–634.

Dewitte W, Riou-Khamlichi C, Scofield S, Healy JM, Jacqmard A, Kilby NJ, Murray JAH. 2003. Altered cell cycle distribution, hyperplasia, and inhibited differentiation in Arabidopsis caused by the D-type cyclin CYCD3. *Plant Cell* **15**: 79–92.

Dhondt S, Van Haerenborgh D, Van Cauwenbergh C, Merks RMH, Philips W, Beemster GTS, Inzé D. 2012. Quantitative analysis of venation patterns of Arabidopsis leaves by supervised image analysis. *Plant Journal* **69**: 553–563.

Donnelly PM, Bonetta D, Tsukaya H, Dengler RE, Dengler NG. 1999. Cell cycling and cell enlargement in developing leaves of Arabidopsis. *Developmental Biology* **215**: 407–419.

Efroni I, Eshed Y, Lifschitz E. 2010. Morphogenesis of simple and compound leaves: a critical review. *Plant Cell* **22**: 1019–1032.

Eloy NB, de Freitas Lima M, Van Damme D, Vanhaeren H, Gonzalez N, De Milde L, Hemerly AS, Beemster GTS, Inzé D, Ferreira PCG. 2011. The APC/C *subunit 10* plays an essential role in cell proliferation during leaf development. *Plant Journal* **68**: 351–363.

Fiorani F, Beemster GTS. 2006. Quantitative analyses of cell division in plants. *Plant Molecular Biology* **60**: 963–979.

Friedrichsen DM, Joazeiro CAP, Li J, Hunter T, Chory J. 2000. Brassinosteroid-insensitive-1 is a ubiquitously expressed leucine-rich repeat receptor serine/threonine kinase. *Plant Physiology* **123**: 1247–1255.

Friml J, Vieten A, Sauer M, Weijers D, Schwarz H, Hamann T, Offringa R, Jürgens G. 2003. Efflux-dependent auxin gradients establish the apical-basal axis of Arabidopsis. *Nature* **426**: 147–153.

Fujioka S, Li J, Choi Y-H, Seto H, Takatsuto S, Noguchi T, Watanabe T, Kuriyama H, Yokota T, Chory J *et al.* 1997. The Arabidopsis *deetiolated2* mutant is blocked early in brassinosteroid biosynthesis. *Plant Cell* **9**: 1951–1962.

Gonzalez N, De Bodt S, Sulpice R, Jikumaru Y, Chae E, Dhondt S, Van Daele T, De Milde L, Weigel D, Kamiya Y *et al.* 2010. Increased leaf size: different means to an end. *Plant Physiology* **153**: 1261–1279.

Gonzalez N, Vanhaeren H, Inzé D. 2012. Leaf size control: complex coordination of cell division and expansion. *Trends in Plant Science* **17**: 332–340.

González-García MP, Vilarrasa-Blasi J, Zhiponova M, Divol F, Mora-García S, Russinova E, Caño-Delgado AI. 2011. Brassinosteroids control meristem size by promoting cell cycle progression in Arabidopsis roots. *Development* **138**: 849–859.

Gudesblat GE, Russinova E. 2011. Plants grow on brassinosteroids. *Current Opinion in Plant Biology* **14**: 530–537.

Hacham Y, Holland N, Butterfield C, Ubeda-Tomas S, Bennett MJ, Chory J, Savaldi-Goldstein S. 2011. Brassinosteroid perception in the epidermis controls root meristem size. *Development* **138**: 839–848.

Hellemans J, Mortier G, De Paepe A, Speleman F, Vandesompele J. 2007. qBase relative quantification framework and software for management and automated analysis of real-time quantitative PCR data. *Genome Biology* **8**: R19.

Hu Y, Bao F, Li J. 2000. Promotive effect of brassinosteroids on cell division involves a distinct *CycD3*-induction pathway in Arabidopsis. *Plant Journal* **24**: 693–701.

Ibañes M, Fàbregas N, Chory J, Caño-Delgado AI. 2009. Brassinosteroid signaling and auxin transport are required to establish the periodic pattern of Arabidopsis shoot vascular bundles. *Proceedings of the National Academy of Sciences of the United States of America* **106**: 13630–13635.

Kauschmann A, Jessop A, Koncz C, Szekeres M, Willmitzer L, Altmann T. 1996. Genetic evidence for an essential role of brassinosteroids in plant development. *Plant Journal* **9**: 701–713.

Kazama T, Ichihashi Y, Murata S, Tsukaya H. 2010. The mechanism of cell cycle arrest front progression explained by a KLUH/CYP78A5-dependent mobile growth factor in developing leaves of *Arabidopsis thaliana*. *Plant and Cell Physiology* **51**: 1046–1054.

Li J, Chory J. 1997. A putative leucine-rich repeat receptor kinase involved in brassinosteroid signal transduction. *Cell* **90**: 929–938.

Li J, Nam KH, Vafeados D, Chory J. 2001. *BIN2*, a new brassinosteroid-insensitive locus in Arabidopsis. *Plant Physiology* **127**: 14–22.

Marrocco K, Thomann A, Parmentier Y, Genschik P, Criqui MC. 2009. The APC/C E3 ligase remains active in most post-mitotic Arabidopsis cells and is required for proper vasculature development and organization. *Development* **136**: 1475–1485.

Miyazawa Y, Nakajima N, Abe T, Sakai A, Fujioka S, Kawano S, Kuroiwa T, Yoshida S. 2003. Activation of cell proliferation by brassinolide application in tobacco BY-2 cells: effects of brassinolide on cell multiplication, cell-cycle-related gene expression, and organellar DNA contents. *Journal of Experimental Botany* **54**: 2669–2678.

Nakajima N, Shida A, Toyama S. 1996. Effects of brassinosteroid on cell division and colony formation of Chinese cabbage mesophyll protoplasts. *Japanese Journal of Crop Science* **65**: 125–130.

Nakamura A, Fujioka S, Sunohara H, Kamiya N, Hong Z, Inukai Y, Miura K, Takatsuto S, Yoshida S, Ueguchi-Tanaka M *et al.* 2006. The role of *OsBRI1* and its homologous genes, *OsBRL1* and *OsBRL3*, in rice. *Plant Physiology* **140**: 580–590.

Nakamura M, Naoi K, Shoji T, Hashimoto T. 2004. Low concentrations of propyzamide and oryzalin alter microtubule dynamics in Arabidopsis epidermal cells. *Plant and Cell Physiology* **45**: 1330–1334.

Nakaya M, Tsukaya H, Murakami N, Kato M. 2002. Brassinosteroids control the proliferation of leaf cells of *Arabidopsis thaliana*. *Plant and Cell Physiology* **43**: 239–244.

Oh M-H, Clouse SD. 1998. Brassinolide affects the rate of cell division in isolated leaf protoplasts of *Petunia hybrida*. *Plant Cell Reports* **17**: 921–924.

Oh M-H, Sun J, Oh DH, Zielinski RE, Clouse SD, Huber SC. 2011. Enhancing Arabidopsis leaf growth by engineering the BRASSINOSTEROID INSENSITIVE 1 receptor kinase. *Plant Physiology* **157**: 120–131.

Ohashi-Ito K, Fukuda H. 2003. HD-Zip III homeobox genes that include a novel member, *ZeHB-13* (Zinnia)/*ATHB-15* (Arabidopsis), are involved in procambium and xylem cell differentiation. *Plant and Cell Physiology* **44**: 1350–1358.

Pérez-Pérez JM, Serralbo O, Vanstraelen M, González C, Criqui M-C, Genschik P, Kondorosi E, Scheres B. 2008. Specialization of CDC27 function in the *Arabidopsis thaliana* anaphase-promoting complex (APC/C). *Plant Journal* **53**: 78–89.

Reinhardt B, Hänggi E, Müller S, Bauch M, Wyrzykowska J, Kerstetter R, Poethig S, Fleming AJ. 2007. Restoration of *DWF4* expression to the leaf margin of a *dwf4* mutant is sufficient to restore leaf shape but not size: the role of the margin in leaf development. *Plant Journal* **52**: 1094–1104.

Savaldi-Goldstein S, Peto C, Chory J. 2007. The epidermis both drives and restricts plant shoot growth. *Nature* **446**: 199–202.

Scarpella E, Marcos D, Friml J, Berleth T. 2006. Control of leaf vascular patterning by polar auxin transport. *Genes and Development* **20**: 1015–1027.

Schnittger A, Schöbinger U, Stierhof Y-D, Hülskamp M. 2002. Ectopic B-type cyclin expression induces mitotic cycles in endoreduplicating Arabidopsis trichomes. *Current Biology* **12**: 415–420.

Serralbo O, Pérez-Pérez JM, Heidstra R, Scheres B. 2006. Non-cell-autonomous rescue of anaphase-promoting complex function revealed by mosaic analysis of *HOBBIT*, an Arabidopsis *CDC27* homolog. *Proceedings of the National Academy of Sciences of the United States of America* **103**: 13250–13255.

Skirycz A, Inzé D. 2010. More from less: plant growth under limited water. *Current Opinion in Biotechnology* **21**: 197–203.

Snustad DP, Haas NA, Kopczak SD, Silflow CD. 1992. The small genome of Arabidopsis contains at least nine expressed ß-tubulin genes. *Plant Cell* **4**: 549–556.

Sun Y, Fan X-Y, Cao D-M, Tang W, He K, Zhu J-Y, He J-X, Bai M-Y, Zhu S, Oh E *et al.* 2010. Integration of brassinosteroid signal transduction with the transcription network for plant growth regulation in Arabidopsis. *Developmental Cell* **19**: 765–777.

Szekeres M, Németh K, Koncz-Kálmán Z, Mathur J, Kauschmann A, Altmann T, Rédei GP, Nagy F, Schell J, Koncz C. 1996. Brassinosteroids rescue the deficiency of *CYP90*, a cytochrome P450, controlling cell elongation and de-etiolation in Arabidopsis. *Cell* **85**: 171–182.

Tsukaya H. 2002. Interpretation of mutants in leaf morphology: genetic evidence for a compensatory system in leaf morphogenesis that provides a new link between cell and organismal theories. *International Review of Cytology* **217**: 1–39.

Tsukaya H. 2005. Leaf shape: genetic controls and environmental factors. *International Journal of Developmental Biology* **49**: 547–555.

Tsukaya H. 2006. Mechanism of leaf-shape determination. *Annual Review of Plant Biology* **57**: 477–496.

Ulmasov T, Murfett J, Hagen G, Guilfoyle TJ. 1997. Aux/IAA proteins repress expression of reporter genes containing natural and highly active synthetic auxin response elements. *Plant Cell* **9**: 1963–1971.

Van Esse GW, Westphal AH, Surendran RP, Albrecht C, van Veen B, Borst JW, de Vries SC. 2011. Quantification of the brassinosteroid insensitive1 receptor in planta. *Plant Physiology* **156**: 1691–1700.

Vanneste S, Coppens F, Lee E, Donner TJ, Xie Z, Van Isterdael G, Dhondt S, De Winter F, De Rybel B, Vuylsteke M *et al.* 2011. Developmental regulation of CYCA2s contributes to tissue-specific proliferation in Arabidopsis. *EMBO Journal* **30**: 3430–3441.

Völker A, Stierhof Y-D, Jürgens G. 2001. Cell cycle-independent expression of the *Arabidopsis* cytokinesis-specific syntaxin KNOLLE results in mistargeting to the plasma membrane and is not sufficient for cytokinesis. *Journal of Cell Science* **114**: 3001–3012.

Wang Z-Y, Seto H, Fujioka S, Yoshida S, Chory J. 2001. BRI1 is a critical component of a plasma-membrane receptor for plant steroids. *Nature* **410**: 380–383.

Weingartner M, Criqui M-C, Mészáros T, Binarova P, Schmit A-C, Helfer A, Derevier A, Erhardt M, Bögre L, Genschik P. 2004. Expression of a nondegradable cyclin B1 affects plant development and leads to endomitosis by inhibiting the formation of a phragmoplast. *Plant Cell* **16**: 643–657.

Wenzel CL, Schuetz M, Yu Q, Mattsson J. 2007. Dynamics of *MONOPTEROS* and PIN-FORMED1 expression during leaf vein pattern formation in *Arabidopsis thaliana*. *Plant Journal* **49**: 387–398.

Wu S, Scheible W-R, Schindelasch D, Van Den Daele H, De Veylder L, Baskin TI. 2010. A conditional mutation in *Arabidopsis thaliana* separase induces chromosome non-disjunction, aberrant morphogenesis and cyclin B1;1 stability. *Development* **137**: 953–961.

Yin Y, Wang Z-Y, Mora-Garcia S, Li J, Yoshida S, Asami T, Chory J. 2002. BES1 accumulates in the nucleus in response to brassinosteroids to regulate gene expression and promote stem elongation. *Cell* **109**: 181–191.

Yoshizumi T, Nagata N, Shimada H, Matsui M. 1999. An Arabidopsis cell cycle- dependent kinase-related gene, *CDC2b*, plays a role in regulating seedling growth in darkness. *Plant Cell* **11**: 1883–1895.

Yu X, Li L, Zola J, Aluru M, Ye H, Foudree A, Guo H, Anderson S, Aluru S, Liu P *et al.* 2011. A brassinosteroid transcriptional network revealed by genome-wide identification of BESI target genes in *Arabidopsis thaliana*. *Plant Journal* **65**: 634–646.

Supporting Information

Additional supporting information may be found in the online version of this article.

Fig. S1 Brassinosteroids promote differentiation.

Fig. S2 Brassinosteroids affect cell division rate in the leaf.

Fig. S3 Brassinosteroids regulate cell proliferation, expansion and differentiation in the leaf.

Fig. S4 Immunodetection of KNOLLE and CDKA;1 in protein extracts from Col-0, *CYCD3;1*^{OE}, *cpd*, and *cpd*;*CYCD3;1*^{OE} leaves.

Fig. S5 Brassinosteroids are required for the onset of differentiation.

Fig. S6 Brassinosteroid signaling fine-tunes leaf growth.

Table S1 List of primers used in this study

Please note: Wiley-Blackwell are not responsible for the content or functionality of any supporting information supplied by the authors. Any queries (other than missing material) should be directed to the *New Phytologist* Central Office.